**FINAL REPORT**

Grant #: 1 R03 OH009381

Dates: 07/01/08 - 06/31/11

Title: A Personal Sampler for Assessing Inhaled Nanoparticle Exposures

Contact: John Volckens, Principal Investigator
Department of Environmental and Radiological Health Sciences
College of Veterinary Medicine and Biomedical Sciences
Colorado State University
1681 Campus Delivery
Fort Collins, Colorado 80523-1681
Phone: (970) 491-6341
Facsimile: (970) 491-2940
john.volckens@colostate.edu

Table of Contents

**List of Figures**

Abstract

Engineered nanoparticles possess unique properties that present potential health risks to the workers who manufacture them and to consumers who are directly or inadvertently exposed to them. Monitoring personal exposures to these materials is necessary to evaluate such potential risks.

This project had three specific aims:

**Specific Aim 1: Design and construct a prototype instrument capable of collecting personal, breathing-zone samples of airborne nanoparticles as a function of time.**

Results: A thermal precipitator was designed to measure concentrations of airborne nanoparticles in the breathing zone of exposed individuals. The prototype is small and lightweight, making it sufficient for personal, breathing-zone use. This device, however, was designed to collect a time-integrated sample, since the use of a rotating substrate was deemed impractical during development and testing.

**Specific Aim 2: Develop a method to estimate personal exposure to airborne nanoparticle number, surface area, and mass concentration over time.**

Results: Particle collection efficiency was evaluated in the laboratory for this device at flow rates of 5 and 20 mL/min and for particle sizes ranging from 15 to 240 nm. Particle transmission efficiency (with the temperature gradient off) and uniformity of particle deposition across the collection surface were also evaluated. Particle collection efficiency ranged from 100% at 5 mL/min flow to approximately 50% at 20 mL/min. We used scanning electron microscopy (SEM) to image, size, and count particles collected by this device. Particle collection was generally homogeneous near the center the collection plate over a distance of approximately 2 mm. Particle collection was less uniform near the edges of the collection plate, with a tendency for increased deposition near the inlet and flow centerline. Knowing the number and size of collected particles, along with instrument flowrate and collection efficiency, we may then determine exposure concentrations as a function of particle size.

**Specific Aim 3: Evaluate the method's ability to identify *engineered nanoparticles* present within an aerosol of mixed origin (i.e., a heterogeneous particle mix).**

Results: We used energy-dispersive spectroscopy to characterize the physio-chemical properties of individual particles sampled from a mixture of two sources: copper welding fume (an incidental nanoparticle) and engineered copper-tin-zinc nanoparticles. Individually-collected particles were differentiated under SEM examination, which demonstrated the validity of this technique for distinguishing engineered nanoparticles from other types of nanoparticles collected from air.

The device engineered from this work will improve our ability to assess worker exposure to engineered nanoparticles. Such a measurement can help establish whether there are links between occupational exposure to engineered nanoparticles and disease, thereby increasing the predictive power of epidemiology and risk assessment. Results from this research can also be translated to the larger realm of health-related air pollution outside of the workplace (*e.g.*, other natural and anthropogenic aerosols).

**SECTION 1.**

Highlights/Significant Findings

A thermal precipitator was designed to measure concentrations of airborne nanoparticles in the breathing zone of exposed individuals. The prototype is small and lightweight, making it sufficient for personal, breathing-zone use. Particle collection efficiency at a flow rate of 5 mL/min was nearly 100% for particle sizes ranging from 15 to 240 nm. Particle collection was generally homogeneous near the center the collection plate over a distance of approximately 2 mm. We used energy-dispersive spectroscopy to characterize the physio-chemical properties of individual particles sampled from a mixture of two sources: copper welding fume (an incidental nanoparticle) and engineered copper-tin-zinc nanoparticles. Individually-collected particles were differentiated under SEM examination, which demonstrated the validity of this technique for distinguishing engineered nanoparticles from other types of nanoparticles collected from air.

Translation of Findings

We disseminated the results of our research at national meetings and through the publication of a manuscript in the peer-review literature. We have also partnered with RJLee Group Inc., a leader in SEM particle analysis, to commercialize this technology. Therefore, the technology developed from this project should soon be available for use by occupational health practitioners worldwide.

Outcomes/Relevance/Impact

This research developed a method to estimate human exposures to engineered nanoparticles in workplace environments. Such a method is critical to the establishment of nanoparticle dose-response relationships, as current methods lack both specificity and sensitivity. A particularly impactful result of this work is that our technique is capable of distinguishing engineered nanoparticles from those of incidental and biogenic origin. Such capability will lead to a better understanding of human exposure to engineered nanoparticles in the workplace, allowing for more effective exposure intervention and the development and evaluation of effective control techniques. Such actions will ultimately lead to improved worker health in the nanotechnology sector.

**SECTION 2 – Scientific Report**

Specific Aims

The growing introduction of engineered nanoparticles in the workplace continues to place workers at risk. While the adverse effects of ultrafine particles on the human cardiopulmonary system are known [1-5], relatively little understanding has been developed regarding the hazards that engineered nanoparticles may present to humans. Elucidation of potential nanoparticle exposure-disease relationships requires the development of an adequate exposure assessment method, as exposure assessment provides key input into subsequent epidemiologic and toxicological investigation. The absence of a personal exposure assessment method for nanoparticle aerosols prevents progress towards understanding potential nanoparticle exposure-disease relationships.

The goal of this work is to develop an accurate, sensitive, and specific method to assess personal exposures to engineered nanoparticles. The method will assess the inhalation route of exposure, and hence, the measurement of nanoparticle concentrations in air. To quantify concentrations of airborne nanoparticles, a measurement must be able to segregate the aerosol by size (to capture only particles smaller than 100 nm) and count these particles following size-segregation. Also, because *inhaled* nanoparticles enter strictly through the oral/nasal route, the method should be oriented to measure *breathing zone* concentrations within the vicinity of the upper torso. Finally, and perhaps most importantly, the method must be able to distinguish *engineered* nanoparticles from other *incidental* nanoparticles (i.e., ultrafine particles) that are ubiquitous in workplace and ambient air.

**Specific Aim 1: Design and construct a prototype instrument capable of collecting personal, breathing-zone samples of airborne nanoparticles as a function of time.**

Approach: A new tool is needed for estimating human exposures to engineered nanoparticles in the workplace. We will design a *thermal precipitator* to capture airborne nanoparticles on a rotating substrate to obtain time-resolved samples, allowing exposure reconstruction with minute-to-hour resolution. The prototype will be small and lightweight for personal, breathing-zone use.

**Specific Aim 2: Develop a method to estimate personal exposure to airborne nanoparticle number, surface area, and mass concentration over time.**

Hypothesis 1: Human exposures to nanoparticle aerosols may be reconstructed using electron microscopy (e.g., SEM, TEM, AFM) techniques to image, size, and count collected particles. Knowing the number and size of collected particles, along with instrument flowrate and collection efficiency, we may determine exposure concentrations as a function of particle size. Furthermore, by collecting these nanoparticles on a moving substrate (discussed below), we may resolve an individual's exposure in time.

**Specific Aim 3: Evaluate the method's ability to identify *engineered nanoparticles* present within an aerosol of mixed origin (i.e., a heterogeneous particle mix).**

Hypothesis 2: *Engineered* nanoparticles can be identified and distinguished from *incidental* and *biogenic* nanoparticles based on the use of energy-dispersive spectroscopy conducted directly on collected particles. By characterizing the physio-chemical properties of individual particles, we will differentiate engineered nanoparticles from other types of nanoparticles and quantify concentrations of each.

## Introduction

As new nanotechnologies develop, there is a growing concern about the adverse health risks that engineered nanoparticles may pose to both humans and the environment [6,7]. Engineered nanoparticles are materials designed on the molecular scale with at least one dimension measuring less than 100 nm. These particles often possess material properties that are enhanced due to their small size. Unfortunately, the same unique properties that make engineered nanoparticles so desirable also make them potentially dangerous [6,8]. Very little human exposure data exist for these particles, although they are known enter the body through a number of routes (e.g., respiration, dermal penetrations, and ingestion). The health implications of inhaled nanoparticle exposure is a particularly important research area as the use of engineered nanoparticles is expected to increase dramatically [9-11], resulting in growing numbers of exposed individuals in both the manufacturing and consumer segments of the population. Nanoparticles may pose significant health concerns because their high surface to volume ration makes them more reactive in biological systems [9]. Once deposited in the respiratory tract, nanoparticles can also translocate between organ systems by virtue of their size [12,13]. For example, nanoparticles deposited in the nose have been shown to reach the brain directly via olfactory and trigeminal nerve axons [14].

However, there is uncertainty surrounding the appropriate metric for characterizing inhaled nanoparticle exposures (i.e., whether particle size, surface area, or composition is the dominant factor in determining toxicity). Nanoparticles vary in size, shape, composition, charge, crystallinity, solubility, and impurities, with potential toxicities likely depending on a combination of factors [15]. Engineered nanoparticles are typically generated monodisperse, however, human exposure can occur to both individual particles and their agglomerates. Current technologies for nanoparticle exposure assessment include methods to determine particle number concentration, particle size distribution [16], particle mass, particle surface area [17], or a combination of these metrics [18-20].

The issue of *specificity* (i.e., particle identification and source attribution) is critical for engineered nanoparticle exposure assessment, as both biogenic (i.e., naturally produced) and incidental (i.e., anthropogenic, non-engineered) nanoparticles, such as those from fossil-fuel combustion, are omnipresent in both indoor and outdoor air. Therefore, methods for engineered nanoparticle exposure assessment should also be capable of differentiating engineered nanoparticles from other aerosols that could potentially confound a measurement. Several studies have used scanning electron microscopy (SEM) and transmission electron microscopy (TEM) to image nanoparticles collected on a variety of substrates, allowing for characterization of various physiochemical particle characteristics [10,20-23]. For example, Miller et al. (2010) developed a hand-held electrostatic precipitator to sample airborne nanoparticles onto a SEM substrate with 74-94% efficiency. The advantage of electron microscopy is that it may be coupled to energy dispersive techniques (e.g., EELS, EDX) to identify particle composition, in addition to size, concentration, and shape.

The state-of-the-art for human exposure assessment to aerosol hazards calls for *personal* sampling, whereby measures are made within the breathing zone of an exposed individual [24]. Personal sampling also accounts for spatial and temporal variation in an individual's exposure in ways that area monitoring cannot [19]. A personal sampler must be small, lightweight, and portable so that it may be mounted to an individual without substantial hindrance. A personal sampler should also be sufficiently inexpensive to facilitate widespread use [6]. With these considerations in mind, we developed a small thermal precipitator to deposit particles onto an electron microscopy grid, allowing for nanoparticle characterization and personal exposure assessment as a function of particle size, composition, and ultimately concentration.

Materials and Methods

### Thermophoretic Aerosol Sampling Theory

Thermal precipitators use thermophoretic force generated from an applied temperature gradient (orthogonal to the aerosol flow) to separate particles from a moving airstream. The temperature gradient is typically created within a shallow flow channel, wherein one side is heated and the other side is cooled. Because of this gradient, gas molecules on one side of the particle have greater kinetic energy than those on the opposite side. Molecules on the hotter side transfer more net momentum per collision, resulting in a *thermophoretic* force on the particle in the direction of decreasing temperature gradient.

The thermophoretic velocity, $V_{th}$, for particles with diameters smaller than the gas mean free path (~66 nm at room temperature and pressure) is independent of particle size and is estimated by:

$$V_{th} = \frac{-0.55\eta\nabla T}{\rho_g T} \quad (1)$$

where η is the viscosity of the gas, $\rho_g$ is the density of the gas, $T$ is the local temperature and $\nabla T$ is the temperature gradient (Waldmann and Schmitt 1966). Larger particles ($d_p$ > 100 nm) develop an internal temperature gradient, resulting in a more complex equation for the thermophoretic force, which results in somewhat smaller thermophoretic velocities (Cohen and Mcammon 2001). Flow through the collection chamber is laminar to minimize loses to surfaces other than the cold plate (flow Reynolds number < 2000). Thermophoretic aerosol samplers have several advantages: the components to create and maintain the temperature gradient are inexpensive, they require relatively simple electronics, and they can use an electron microscopy substrate as the collection surface. The main disadvantage is that this technique is not direct-reading, requiring a time-integrated sample and subsequent laboratory analysis.

### 2009 Prototype

In 2009, a prototype thermophoretic personal sampler was designed, built, and tested by a team of mechanical engineering students at Colorado State University as their senior design project. The device was designed to collect airborne nanoparticles onto eight TEM grids over an eight hour work shift. Sampled aerosol was directed over each individual grid by rotating the flow exit in a semi-circular path about the collection chamber. The grids were mounted on magnets placed in a cooled aluminum plate, and the flow path was rotated across a new grid each hour. The TEM grids could then be removed for analysis to determine morphology, chemical makeup, and concentration. A 3D model and photograph of this prototype device is presented in Figure 1.

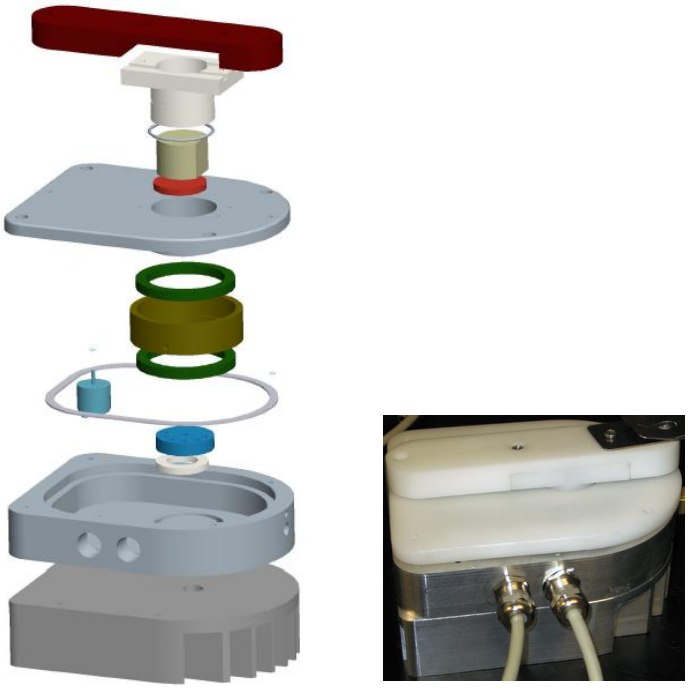

**Figure 1. Three-dimensional model and photograph of the 2009 Colorado State University Senior Design Team thermophoretic sampler prototype.**

The initial prototype had several serious drawbacks. The device was too large and cumbersome to be acceptable for personal use. The thermophoretic sampler measured approximately 12.7 by 10.2 by 7.5 cm and weighed 901.4 g. The controller, batteries, and pump occupied a large volume and were contained in a backpack, separate from the thermophoretic sampler. The electrical circuitry was not optimized as the system required three separate batteries to supply power to the thermoelectric cooler, heater, and controller. Lead-acid batteries were used, which are relatively inexpensive, but very heavy, weighing a total of 2.6 kg. In addition, the device had large power requirements and therefore large batteries with the capacity to operate for 6-8 hours (a typical work shift) were necessary. Ideally, the sampler should be powered with a single, lightweight battery.

A fluid flow simulation of this device using FLUENT modeling software (Ansys, Inc., Ann Arbor, Michigan) also revealed problems with contamination within the sample collection zone. A particle track simulation of the sample collection zone is shown in Figure 2. This simulation shows the paths of particles colored as a function of time in the collection chamber. The two large circles represent the hot and cold plates (top and bottom, respectively). The two small circles represent the inlet to the sampler and the small rectangle represents the outlet. The particles cross multiple collection surfaces, which would give misleading results during subsequent TEM analysis of the grids.

Leak tests also revealed that the device did not seal upon application of a vacuum. A pneumatically-

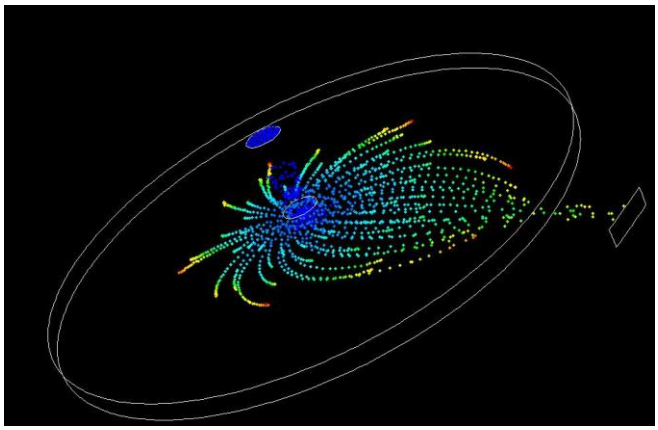

**Figure 2. Fluent computer simulation of particle transport within the 2009 prototype showing aerosol dispersion within the collection zone.**

sealed collection chamber is essential to prevent contamination and unwanted airflow during instrument operation and handling.

In light of the issues associated with this first prototype, we decided to develop a second prototype that collected only a time-integrated sample onto a single collection substrate. Although this second prototype lacked the time-resolved features proposed under Aim 1, we decided that alleviation of the aforementioned issues was critical to the overall success of the research.

Therefore, a new, simpler device was designed and tested. The new sampler was smaller and lighter than the original design. Because of reduced power needs, it requires only a single, lightweight battery to power all of its electrical systems.

### 2010 Prototype

The prototype thermal precipitator measures 5.0 cm by 5.0 cm by 7.4 cm (L x W x H), weighs 222.4 g, and consumes approximately 7.2 W of power during normal operating conditions (Figure 3). Power is supplied to the device using a rechargeable, 12-V lithium-ion battery and a custom, high efficiency power circuit (Analog Devices, Inc., Fort Collins, CO). The battery (678 g) and controller (100 g) are connected to the device using a cat5e cable so that these heavier components can be worn on a belt (along with a personal sampling pump), while the sampler is mounted within the breathing zone (Figure 3).

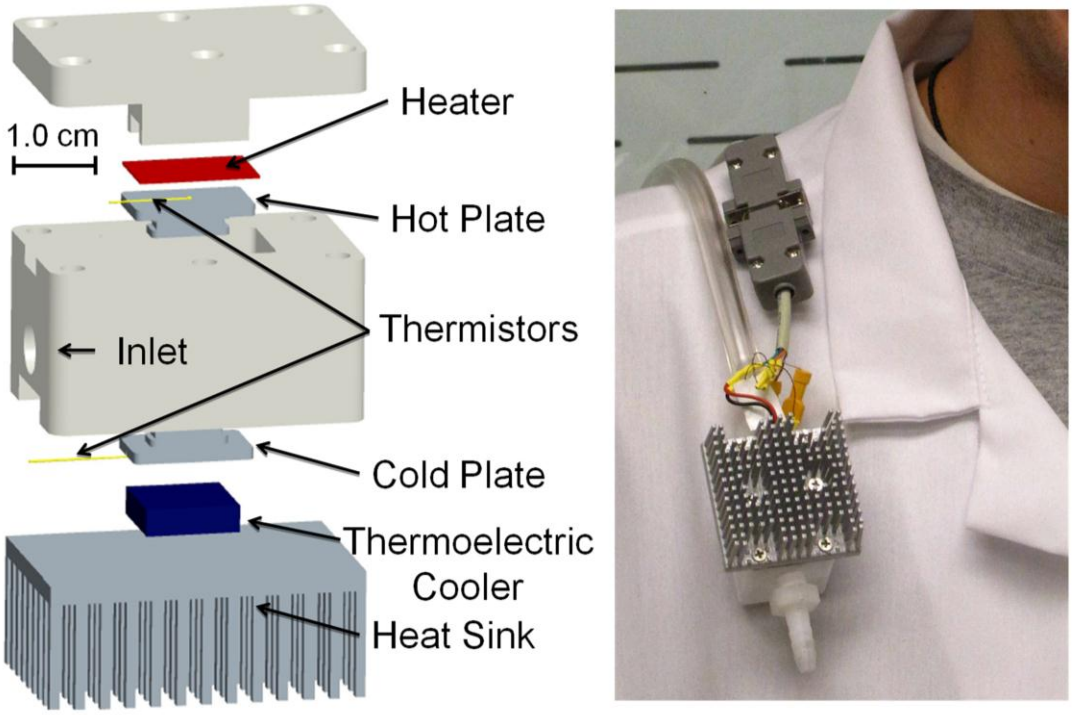


**Figure 3. Exploded diagram and photograph of the 2010 prototype thermophoretic aerosol sampler.**

The collection surface (i.e. the aluminum cold plate in Figure 3, $T$=12.2°C) measures 13 mm by 5 mm, and is cooled with a small, low-power thermoelectric cooler (TE Technology Inc., Traverse City, MI). A hot plate ($T$=122°C) of identical dimensions is located 1 mm above the cold plate and is heated with a 0.10 mm diameter Nichrome wire heater. This heater is insulated from other components with 0.0254 mm thick polyimide (Kapton) plastic adhesive sheets. The chamber inlet measures 5 mm wide by 1 mm high to match the plate width and separation distance, respectively. The 1 mm separation distance was chosen to maximize the temperature gradient while maintaining reasonable tolerances for machining and assembly of the components. The temperatures of the cold and hot plates are maintained via a

programmable temperature controller (Analog Devices, Inc., Fort Collins, CO) in conjunction with two small thermistors. The hot plate temperature was constrained to 122˚C for safety considerations. The cold plate temperature (12.2 °C) was chosen to minimize condensation during a sampling event, while maximizing the temperature gradient (100˚C/mm). A small heat sink dispersed heat generated by the thermoelectric cooler.

Based on Equation 1 and a flow rate of 5 mL/min, we estimated a path length of 8-10 mm required for a theoretical unit density particle entering the device at a height of 1 mm above the collection surface (the plate separation distance) to deposit (depending on the temperature used in Equation 1) under a temperature gradient of 100 °C/mm. Since the collection plate is 13 mm long, 100% collection efficiency was expected for the device at this flow rate. At a sample flow rate of 20 mL/min, the deposition distance will increase to 35-40 mm, resulting in a collection efficiency around 35% (assuming a uniform particle concentration distribution across the inlet face). The Reynolds numbers (for both the particle and the flow) are laminar under these conditions. Nickel transmission electron microscope grids are held in place with an inlaid magnet on the cold plate.

Two other thermal precipitator designs have been reported in the literature for nanoparticle measurement. Azong-Wara et al. (2009) developed and modeled a thermal precipitator that operated at 2 mL/min with a 15 ˚C/mm temperature gradient at a spacing of 1 mm. Modeling results indicated that the deposition of particles should be uniform across the collection plate, reducing the number of images required to determine the ambient concentration. However, this design has yet to be evaluated in the laboratory to our knowledge. Lorenzo et al. (2007) developed and tested a device that operates at 2 L/min with a 400 ˚C/mm temperature gradient at a plate spacing of 0.3 mm. Those authors were able to reproduce the particle size distribution from TEM images with good agreement to existing size distribution measurement systems (i.e., electrical mobility sizing).

### Collection Efficiency and Transmission Efficiency Tests

To evaluate the performance of the thermal precipitator, a series of experiments were conducted to measure particle collection efficiency, particle transmission losses, and to determine the uniformity of particle deposition across the collection surface. The collection efficiency is defined as the percentage of particles entering the thermal precipitator that are collected while the temperature gradient is established. The transmission losses are defined as the percentage of particles entering the thermal precipitator that are collected while there is no temperature gradient (upper limit estimate of losses in the device due to particle diffusion and, to a lesser extent, settling). The particle deposition uniformity tests were conducted to determine the most representative location for electron microscopy analysis of collected particles. The setup used for these procedures is shown in Figure 4.

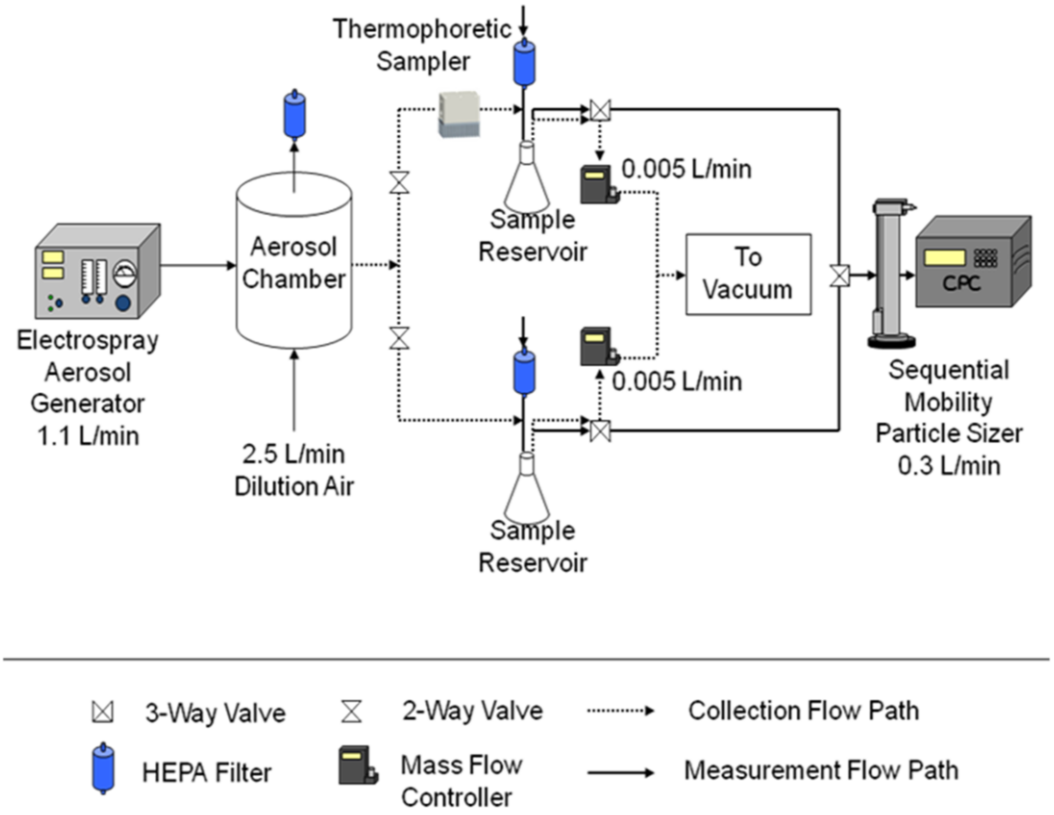


**Figure 4. Experimental setup for the collection efficiency tests.**

Particle collection efficiency was calculated from the difference in particle concentration measured between two parallel sampling lines: one line containing the thermal precipitator and an identical line that served as a control. However, since typical reference instruments cannot operate at the low flow rate of the thermal precipitator (5 or 20 mL/min), a pair of 2 L delay reservoirs were placed immediately downstream of the parallel measurement lines (Figure 4). These sample reservoirs were initially cleared of contaminating aerosol. Nanometer-sized, monodisperse test aerosols ($d < 100$ nm) were created from a sucrose solution using an electrospray aerosol generator (TSI Inc., Shoreview, MN). Larger test aerosols ($d > 100$ nm) were generated using an atomized solution containing polystyrene latex (PSL) spheres (Duke Scientific Corp., Palo Alto, CA). Test aerosol was sent to a dilution chamber, mixed with dry air, and then directed into the two parallel sampling lines. These two lines were identical in length and kept as straight as possible to minimize particle losses. Initial tests without the thermal precipitator in line demonstrated that aerosol concentrations measured between the two parallel lines were within 10% of each other. The thermal precipitator was placed in line and immediately upstream of one reservoir, while the parallel line contained a second reservoir to act as a control. The precipitator was operated with the heated plate on top to minimize thermal convection; however, modeling studies of thermal precipitators have found that the orientation of the collection plates has minimal effect on instrument performance (Azong-Wara et al. 2009). Aerosol flow to the sample reservoirs was applied with laboratory vacuum and regulated using mass flow controllers (Omega Engineering, Inc). The variance in the measured flow rate was 20% at 5 mL/min and 1% at 20 mL/min. The reservoirs were filled for 3-5 hours for PSL to generate sufficient concentrations for measurement. The electrospray generated very high concentrations of particles, so collection tests lasted as little as 20 minutes. After a sufficient sampling time, a sequential mobility particle sizer (SMPS, GRIMM Technology) was used to measure size-specific aerosol concentrations in each reservoir, with multiple measurements alternating between reservoirs. The collection efficiency of the thermal precipitator was calculated from the

differential concentrations between the sample reservoirs. At least three replicate tests were conducted for each flow rate and particle size.

All statistical tests were conducted using Matlab software (The Mathworks, Inc., Natick, MA) with an assumed Type 1 error rate (alpha) of 0.05. Tukey's method for multiple comparisons among means was used to determine whether significant differences existed for particle collection efficiencies as a function of particle size. Confidence intervals for the difference in means for each pair-wise comparison were calculated. Box-Cox tests were conducted on all data sets and data were log transformed, when necessary, to satisfy model assumptions of normality and homoscedasticity

### Deposition Uniformity Tests

A third set of tests was conducted to determine the uniformity of particle deposition across the surface of the collection plate. For these tests, the same procedure for the collection efficiency tests was used but the parallel sample reservoir was removed. Each test was conducted for 6 hours, using a 0.1% salt solution aerosolized from a Collison nebulizer, which produced a polydisperse aerosol with an average count median diameter of 30.8 nm and an average geometric standard deviation of 2.0. Polydisperse aerosol was used so that all sizes could be analyzed with a single experiment to minimize the time required for SEM analysis. After particle collection, the cold plate was removed from the device and systematically imaged using a field-emission scanning electron microscope (JSM-6500F, JEOL Inc., Peabody, MA). A series of ten SEM images was taken across the width of the collection plate at distances of 2, 3.75, 5.5, 7.25, and 9 mm downstream of the inlet (50 images total). Deposition uniformity tests were repeated twice.

After imaging the particles under the SEM, the surface concentration of deposited particles on the collection plate was determined using ImageJ (Rasband 2009) software for three projected area diameter ranges: 20 to 50, 50 to 100, and 100 to 200 nm (see Supplemental Material for additional information). Measured surface concentrations of deposited particles (i.e., the number of particles counted in a given image) were normalized to the average number of particles per image counted across the entire plate. This normalization step allowed data from replicate experimental runs to be pooled. Particle deposition uniformity (i.e. the percent deviation from the number of particles in a given image compared to the mean number of particles depositing to all regions of the plate) was calculated at each location. A contour plot was constructed to visualize the uniformity of deposited particle surface concentration as a function collection plate region and particle size. Additionally, deposition reproducibility (i.e., whether these uniformity tests were reproducible) was evaluated though multiple repeat tests.

### Particle Identification Test

The final aim of this project was to establish whether energy-dispersive techniques could distinguish between *incidental* and *engineered* nanoparticles collected simultaneously by this device. For this work, a suspension of engineered copper-tin-zinc nanoparticles (Prieto Battery, Fort Collins, CO) was nebulized into an aerosol chamber that contained copper welding fume generated from a portable spot welder. Generated particle size distributions and concentrations were controlled to make them as similar as possible. The thermophoretic device then sampled these aerosols for a 2 hr period. Collected samples were analyzed for elemental signatures using scanning electron microscopy coupled to energy dispersive spectroscopy.

## Results and Discussion

### Collection Efficiency

Particle collection efficiencies as a function of particle diameter for flow rates of 5, 20, and 6.7 mL/min (the latter with zero temperature gradient) are presented in Figure 5. Each point represents the average collection efficiency for three repetitions at each size and flow rate. Error bars represent one standard

deviation. When the thermal precipitator was operated at a flow rate of 5 mL/min, the average collection efficiency for each of the four particle sizes was greater than 99%, with standard deviations less than 1%. This result was expected since the precipitator was designed to collect all particle sizes with 100% efficiency at 5 mL/min. Differences in the length of time of the collection phase of testing had no effect on the collection efficiency for each particle size. Furthermore, there were no significant differences in the collection efficiencies among the various particle sizes ($p = 0.72$). This result was also expected, since the thermophoretic velocity is nearly independent of particle size for diameters less than 100 nm. These results verify that the thermal precipitator is effective at capturing particles from 15 to 240 nm in diameter. Higher collection efficiencies support a more precise exposure assessment by reducing the uncertainty associated with calculating breathing-zone concentrations of airborne nanoparticles.

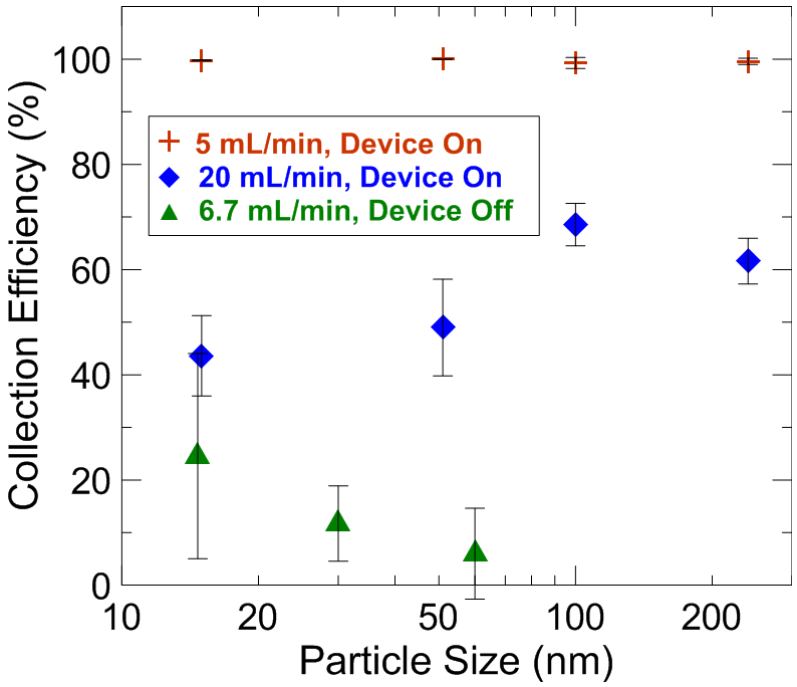


**Figure 5. Measured collection efficiency as a function of particle size, flow rate, and applied temperature gradient (device on vs. off). Error bars represent one standard deviation.**

The total number of particles collected scales with the product of flow rate and collection efficiency, therefore, higher flow rates may be desired, especially if method sensitivity is important. Thus, the collection efficiency at 20 mL/min flow was also investigated. The observed collection efficiencies were reduced by up to a factor of two with the 100 nm collection efficiency significantly larger than for the 15 and 51 nm particles ($p = 0.012$). It is unclear why the collection efficiency is larger for the 100 nm particles than for the smaller particles, as this goes against theory. Reduced particle collection with increased flow was expected. The measured collection efficiency data also had greater variability, and hence greater uncertainty. Therefore, the precipitator is less precise when operated at higher flow rate.

Decreased collection efficiency at an increased flow rate likely resulted from the increase in air velocity and a decrease in residence time for the particles within the collection chamber. As flow rate increases, particles entering the collection chamber have less time to migrate to the collection surface before exiting with the flow at the rear of the chamber. If lower concentrations are anticipated during measurement, the flow rate can be increased (to increase sensitivity, i.e. twice the number of particles would be collected by increasing the flow rate from 5 mL/min to 20 mL/min over a given sampling duration, after accounting for a ~50% reduction in collection efficiency at the higher flow rate) and

correction factors can account for the inefficiency of the thermal precipitator. However, at a higher flow rate, only relatively large differences in the concentration are likely be detected, due to increased uncertainty in particle collection efficiency. Higher flow rates may also be desirable for ease of operation of the thermal precipitator. A wider variety of pumps are available at 20 mL/min and greater flow rates and since the thermal precipitator is intended to be worn as a personal sampler, a small pump that supplies a reliable flow rate is critical to reconstruct personal exposures accurately.

### Transmission Efficiency

Particle collection efficiencies at 6.7 mL/min with the device turned off are also shown in Figure 5. Without an applied temperature gradient, particle collection was highly variable, yet generally less than 25%. This value represents an upper limit to the losses within the thermal precipitator because these collection efficiencies include diffusional deposition onto the lower plate, which is the desired collection surface. Further, since thermophoresis is a special from of Brownian motion, in which the overall, “random” motion from air molecule collisions is directed down the temperature gradient, particles entering near the hot plate would be immediately directed towards the cold plate, reducing the overall losses in the instrument. Aerosol diffusion losses tend to decrease with increasing particle size, since smaller particles are more affected by Brownian motion than larger ones. The losses within the chamber were approximately 25% for very small nanoparticles, but rapidly decrease to relatively low levels (less than 10% of the collection efficiency at a 6.7 mL/min flow rate) for larger particles. However, due to the variability in the data, no significant differences were detected in transmission efficiency as a function of particle size ($p = 0.28$). The increased variability associated with these transmission losses was likely an artifact of using delay reservoirs. The particle concentrations in the reservoirs decrease exponentially as the aerosol is sampled and because only one sequential mobility particle sizer was used, the two reservoirs could not be sampled simultaneously.

### Deposition Uniformity

The uniformity of particle deposition across the collection surface, represented as the relative surface concentration of deposited particles, is shown in Figure 6. Depicted in the figure are relative particle counts (i.e., the number of particles deposited per unit surface area divided by the average number of particles per unit surface area counted across the entire plate). For example, the white contours represent the locations where the deposited particle surface concentration was equal to the average concentration across the plate. Darker contours indicate areas of increased surface deposition; hatched contours represent areas of decreased surface deposition. The median difference in surface deposition concentration was less than 30% (for any given location) among replicate tests.

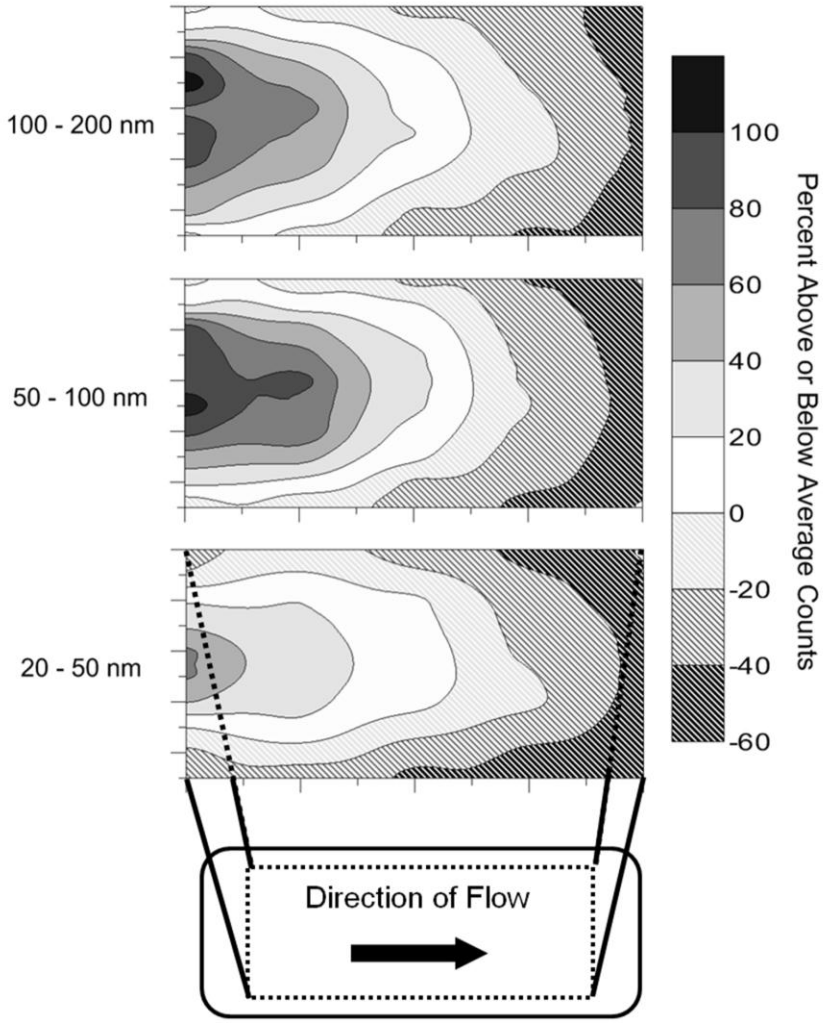


**Figure 6. Uniformity of particle deposition across the collection surface as a function of particle size. Solid and hatched contours represent positive and negative percent deviations from the average surface count (deposited particles/unit area), respectively (white contours represent locations of average surface counts). The x- and y-axes define the area of the particle collection plate, as shown in the inset. Each image represents an average of three tests.**

Collected particles were distributed most densely at the entrance and along the centerline of the collection plate for all three size ranges (Figure 6). The increase in particle counts along the centerline contrasts with data reported by Lorenzo et al. (2007), who found that particles were concentrated at the edges of the collection plate. They attributed this to the parabolic flow profile established in the chamber. However, our design flow rate is about 2% of the flow rate used in their studies, so that even particles moving at higher velocity along the flow centerline have sufficient time to collect. Instead, the increase in particle deposition along the flow centerline may result from a non-uniform temperature gradient in our device. Heat transfer at the boundary between the aluminum plates and the PTFE walls could cause the temperature gradient to decrease away from the center of the plate, which would result in a lower thermophoretic velocity at the chamber edges. The reason for the increased particle deposition near the entrance of the collection chamber is not clear. However, this finding correlates with the greater-than-predicted collection efficiency observed at 20 mL/min.

The relative standard deviation of particle deposition to any location on the cold plate was less than 30% for all three particle sizes, indicating that the relative flux of particles to a given area of the collection plate, although variable, is somewhat repeatable. Therefore, the location of an electron microscopy grid on the collection plate should be chosen based on the measurement need. For

example, a TEM grid placed in the center of the collection plate will provide a sample containing approximately the average number deposited particles per unit surface area over the entire plate. TEM analysis of these grids would provide the best estimate of the true number of sampled particles for exposure assessment. However, a TEM grid placed closer to the inlet of the device would collect more particles (as seen in Figure 4), if increased sensitivity is desired.

### Particle Identification Test

Aerosol number concentrations for the particle identification tests were approximately $2.0 \cdot 10^5$ /cm$^3$ within the test chamber. Both the copper fume and engineered nanoparticle aerosols were approximately log-normal. The copper fume had a median diameter of approximately 70nm and the Cu-Sn-Zn nanoparticle dispersion had a median size of approximately 100 nm. Both aerosols showed substantial overlap in their generated size distributions, as shown in Figure 7.

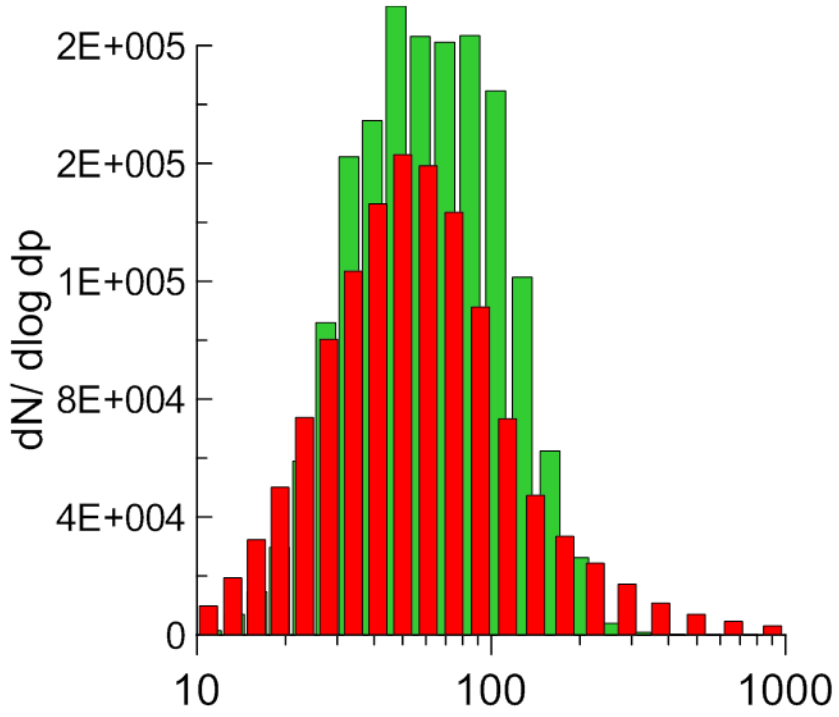


**Figure 7. Generated size distributions of Cu-Sn-Zn nanoparticles (green) and copper welding fume (red). Particle electrical mobility diameter is shown on the x-axis in terms of nanometers.**

Collected particles were examined using SEM-EDX on a Hitachi S-5500 electron microscope at 30 kV. Example scans of two particles are shown below in Figure 8. In this figure, the energy spectra for each particle scan is shown with a bright-field image of the particle itself. As can be seen from the two spectra, both particles show a strong copper peak, but only the particle from the bottom panel gives additional peaks for Zn and Sn, which identifies this particle and an engineered nanoparticle. This result helps demonstrate the power of SEM-EDX for providing *specificity* in nanoparticle identification.

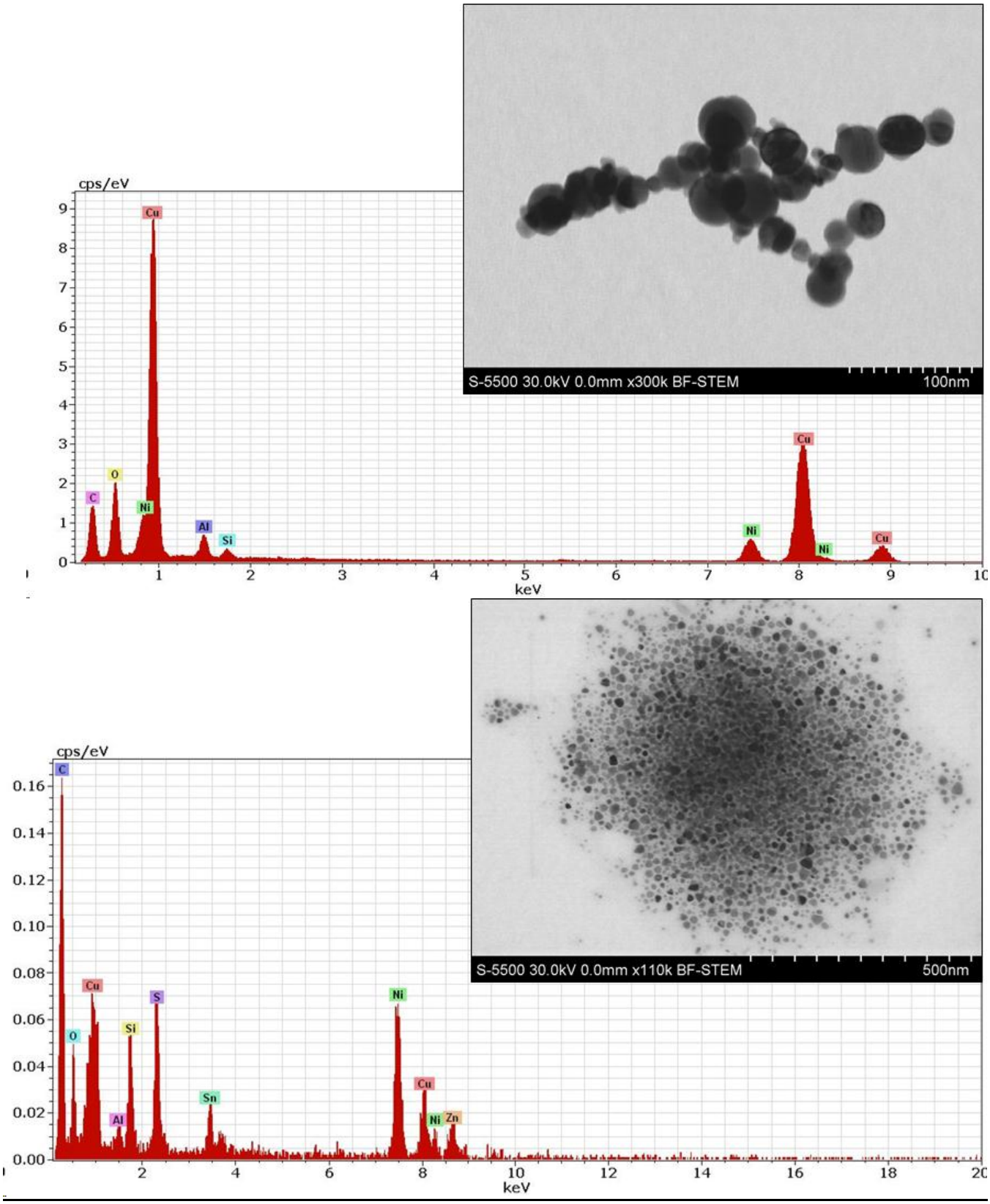


**Figure 8. Comparison of two particles identified using SEM-EDX. The top panel shows a copper fume particle from spot welding; the bottom panel shows a particle with a strong zinc and tin signature, indicated that this particle was engineered.**

Conclusions and Future Work

Personal samplers are needed to estimate human exposure and for use in toxicological studies focusing on inhaled nanoparticles. A personal thermal precipitator was designed and tested to meet this need. Three experiments were conducted to test the performance of the thermal precipitator. Design calculations were verified with experimental collection efficiencies near 100% for test aerosols with 15, 51, 100, and 240 nm diameters. The test was repeated at a flow rate of 20 mL/min to determine the decrease in collection efficiency for a higher flow rate. Increasing the flow rate by a factor of four decreased particle collection efficiency by approximately a factor of two. However, the thermal precipitator's precision decreased dramatically with an increase in flow rate for the 20 mL/min flow rate. Diffusion losses were estimated and measured while the device was turned off (transmission efficiency), so that correction factors could be developed to account for particle losses during sampling.

Particles collected onto the cold plate were also analyzed to determine the homogeneity of collection across the cold plate using scanning electron microscopy and imaging software. Particle collection was generally homogeneous across the center of the collection plate over a distance of approximately 2 mm. This area also coincides with the location where the average number of particles per image was obtained, which represents the ideal location for the placement of a TEM grid. Future testing should be carried out in the field in less controlled environments. Such studies can verify that the thermal precipitator coupled with TEM imaging can be used to distinguish between engineered and incidental nanoparticles and to determine limits of detection for chemical analyses.

Correction factors must also be determined to reconstruct the actual sampled aerosol concentrations from the particle counts obtained from electron microscopy analysis. Calculations using the known flow rate and particle counts from electron microscope images can provide an estimated reconstruction of the concentration measured by the thermophoretic sampler. The calculation results can be compared to the known concentration entering the device to infer a correction factor to account for losses within the device. This is an area for future research. Additionally a suitable pump for personal aerosol sampling should be evaluated to ensure that the proper flow rate can be maintained in the field.

Currently, no standard method exists to characterize personal exposure to engineered nanoparticles, but this technique may provide a feasible option. Impaction is commonly used to for aerosol sampling, but low-pressure methods are necessary to collect nanoparticles, which are not feasible for personal sampling. The National Institute of Occupational Safety and Health (NIOSH) has suggested that nanoparticles can be captured onto a filter and analyzed following the Nanoparticle Emission Assessment Technique (Hodson 2009). However, filters may not be reliable for exposure reconstruction (when imaging methods are used to count and size collected particles) as nanoparticles can penetrate deep into the filter matrix - making quantitative exposure assessment difficult. Even when membrane filters (i.e., Nuclepore) are used, surface collection efficiencies are less than 55% for particles smaller than 100 nm, which collect deep within the filter pore (Cyrs et al. 2010).

At the time of writing this report, Colorado State University is currently partnering with RJLee Group, Inc. to commercialize this technology for sales and distribution in the United States. RJLee Group has secured one year of Phase-1 funding for this endeavor.

Publications From This Work

Journal Articles

Thayer, D., Koehler, K.A., Marchese, A., and J. Volckens. (2011) “A Personal, Thermophoretic Sampler for Airborne Nanoparticles.” Aerosol Science and Technology. 45(6): 734-740. doi: 10.1080/02786826.2011.558943

Proceedings/Presentations

“Laboratory Evaluation of A Personal, Thermophoretic Sampler for Airborne Nanoparticles”. Platform Presentation. American Association for Aerosol Research, Portland, OR, October 2010.

“A Personal, Thermophoretic Sampler for Airborne Nanoparticles.” Poster Presentation. American Industrial Hygiene Conference and Exposition, Denver, CO, May 2010.

“A Personal Sampler for Assessing Inhaled Nanoparticle Exposures.” Platform Presentation. American Industrial Hygiene Conference and Exposition, Toronto, Canada, June 2009.

“Nanoparticle Exposure Assessment: Finding a Needle in a Haystack.” Rocky Mountain Academy of Occupational and Environmental Medicine. Denver, CO, January 2009

Theses

Thayer, D: [2010] “A Personal, Thermophoretic Sampler for Airborne Nanoparticles.” MS Thesis, Department of Mechanical Engineering, Colorado State University, Fort Collins, CO.

Inclusion of gender and minority study subjects

Not applicable.

Inclusion of Children

Not applicable.

Materials available for other investigators

None.

References Cited


1. Kettunen, J., et al., *Associations of fine and ultrafine particulate air pollution with stroke mortality in an area of low air pollution levels.* Stroke, 2007. **38**(3): p. 918-22.
2. Schwarze, P.E., et al., *Particulate matter properties and health effects: consistency of epidemiological and toxicological studies.* Human & Experimental Toxicology, 2006. **25**(10): p. 559-79.
3. Kreyling, W.G., M. Semmler-Behnke, and W. Moller, *Ultrafine particle-lung interactions: does size matter?* Journal of Aerosol Medicine, 2006. **19**(1): p. 74-83.
4. Vinzents, P.S., et al., *Personal exposure to ultrafine particles and oxidative DNA damage.* Environmental Health Perspectives, 2005. **113**(11): p. 1485-90.
5. Delfino, R.J., C. Sioutas, and S. Malik, *Potential role of ultrafine particles in associations between airborne particle mass and cardiovascular health.* Environmental Health Perspectives, 2005. **113**(8): p. 934-46.
6. Maynard, A.D., et al., *Safe handling of nanotechnology.* Nature, 2006. **444**(7117): p. 267-9.
7. Wiesner, M., et al., *Decreasing Uncertainties in Assessing Environmental Exposure, Risk, and Ecological Implications of Nanomaterials.* Environmental Science & Technology, 2009. **43**(17): p. 6458-6462.
8. Thomas, K., et al., *Research strategies for safety evaluation of nanomaterials, Part VIII: International efforts to develop risk-based safety evaluations for nanomaterials.* Toxicological Sciences, 2006. **92**(1): p. 23.
9. Tsuji, J., et al., *Research strategies for safety evaluation of nanomaterials, part IV: risk assessment of nanoparticles.* Toxicological Sciences, 2006. **89**(1): p. 42.
10. Gonzalez, D., et al., *A New Thermophoretic Precipitator for Collection of Nanometer-Sized Aerosol Particles.* Aerosol Science and Technology, 2005. **39**(11): p. 1064 - 1071.
11. Azong-Wara, N., et al., *Optimisation of a thermophoretic personal sampler for nanoparticle exposure studies.* Journal of Nanoparticle Research, 2009. **11**(7): p. 1611-1624.
12. Nemmar, A., et al., *Passage of Intratracheally Instilled Ultrafine Particles from the Lung into the Systemic Circulation in Hamster.* Am. J. Respir. Crit. Care Med., 2001. **164**(9): p. 1665-1668.
13. Oberdorster, G., et al., *Extrapulmonary translocation of ultrafine carbon particle following whole-body inhalation exposure of rats.* Journal of Toxicology and Environmental Health Part A, 2002. **V65**(20): p. 1531.
14. Oberdörster, G., et al., *Translocation of inhaled ultrafine particles to the brain.* Inhalation Toxicology, 2004. **16**(6-7): p. 437-445.
15. Schulte, P., et al., *Issues in the development of epidemiologic studies of workers exposed to engineered nanoparticles.* Journal Of Occupational And Environmental Medicine, 2009. **51**(3): p. 323.
16. Li, L., D.-R. Chen, and P.-J. Tsai, *Use of an electrical aerosol detector (EAD) for nanoparticle size distribution measurement.* Journal of Nanoparticle Research, 2009. **11**(1): p. 111-120.
17. Fissan, H., et al., *Rationale and principle of an instrument measuring lung deposited nanoparticle surface area.* Journal of Nanoparticle Research, 2007. **9**(1): p. 53-59.
18. Demou, E., P. Peter, and S. Hellweg, *Exposure to Manufactured Nanostructured Particles in an Industrial Pilot Plant.* Annals of Occupational Hygiene, 2008. **52**(8): p. 695-706.

19. Brouwer, D.H., J.H.J. Gijsbers, and M.W.M. Lurvink, *Personal Exposure to Ultrafine Particles in the Workplace: Exploring Sampling Techniques and Strategies.* Annals of Occupational Hygiene, 2004. **48**(5): p. 439-453.

20. Peters, T., et al., *Airborne monitoring to distinguish engineered nanomaterials from incidental particles for environmental health and safety.* Journal Of Occupational And Environmental Hygiene, 2009. **6**(2): p. 73-81.

21. Handy, R., et al., *The measurement of ultrafine particles: a pilot study using a portable particle counting technique to measure generated particles during a micromachining process.* Journal of Materials Engineering and Performance, 2006. **15**(2): p. 172-177.

22. Han, J., et al., *Monitoring multiwalled carbon nanotube exposure in carbon nanotube research facility.* Inhalation Toxicology, 2008. **20**(8): p. 741-749.

23. Miller, A., et al., *A Handheld Electrostatic Precipitator for Sampling Airborne Particles and Nanoparticles.* Aerosol Science and Technology, 2010. **44**(6): p. 417-427.

24. Vincent, J.H., *Aerosol Sampling: Science and Practice*. 1989, New York: John Wiley & Sons.